IEEE Robotics and Automation Letters (RA-L) paper, presented at ICRA 2024, Yokohama, Japan. Cite as RA-L paper.

Unified Power and Admittance Adaptation for Safe and Effective Physical Interaction with Unmodelled Dynamic Environments

Federico Benzi and Cristian Secchi

Abstract—**When interacting with unmodelled dynamic systems, a robot controller should be capable of adapting online its behavior, in order to be robust to the changing environmental conditions. In the paradigm of passivity-based control, virtual energy tanks allow to perform such adaptations in a robustly stable way, by bounding the amount of energy allocated to the controller. Nevertheless, when the workspace is shared with human collaborators, additional limits have to be imposed to the power the system can exert, in order to guarantee the overall safety. These bounds are difficult to estimate a priori, might vary over time and can significantly affect task execution. In this letter, we tackle this problem by simultaneously adapting online the admittance and the power limits in the controller, ensuring both safety and task performance. Experimental results with a collaborative manipulator validate the presented framework.**

Index Terms—**Physical Human Robot Interaction, Compliance Control, Robust/Adaptive Control**

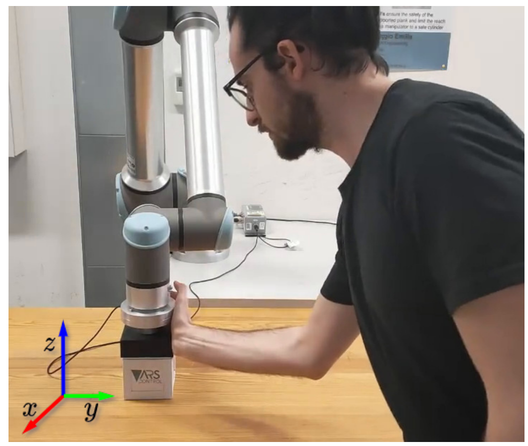

Fig. 1: A collaborative manipulator pushing a box of unknown mass in an unmodelled shared human-robot scenario.

I. INTRODUCTION

MODERN developments in robotics have reignited interest in investigating the physical interaction with complex, dynamic and unknown environments [1], [2]. In this context, energy-based control techniques have shown promising results [3], [4]. By treating the controller and the environment as different subsystems [5] exchanging power among them [6], they allow to properly deal with the uncertainty and variability of the dynamics during the interaction phase. Adopting this framework, it is possible to ascertain the stability of the implemented behavior using passivity criterions [7]. Passivity-based control finds numerous applications in different fields of robotics, such as teleoperation [8], multi-robot systems [9], shared control [10] and collaborative robotics [11], [12].

Among common passivity control techniques, energy tanks [13] have distinguished themselves for their flexibility, as they allow to separate the passivity condition from a specific dynamics. Energy tanks serve as virtual energy storing elements, accumulating the power dissipated over time by the interconnected system and later employing it for passivizing potentially active behaviors. In the context of physical interaction with unmodelled environments, they have been successfully employed for flexible joints robots [14], aerial manipulators [15] and legged manipulators [16], owing to the generality of the energy-based formulation.

Recent works have also highlighted the importance of bounding not only the amount of available energy, but also the rate at which this energy is provided. In [17], the authors introduce the concept of power valves, which limit the extractable power from the ports of the energy tank. This augmentation allows to achieve additional higher-level safety tasks, as showcased in [18] and [19] for aerial manipulators interacting with dynamic environments, and in [20], in which the authors formulate a safety-aware passive variable impedance controller for redundant manipulators operating in shared workspaces. These concepts and methodologies are, in fact, particularly suitable for applications foreseeing Human-Robot Collaboration (HRC), in which the nature of the environment is inherently unstructured and for which providing safety guarantees is a strong necessity.

Yet, all of the aforementioned works consider a fixed value for the maximum power bounds. Since a proper computation of this value would require precise knowledge of the task and of the environment, something unachievable in unstructured scenarios, these value often end up being conservative. This, in turn, strongly undermines the proper execution of the task.

To overcome this issue, in this letter we present an iterative learning control algorithm for simultaneously adapting the admittance dynamics and the exertable power bound of a collaborative manipulator physically interacting with an unmodelled environment, in order to effectively perform a trajectory tracking task. The variation of the admittance dy-

Manuscript received: July 8, 2023; Revised September 21, 2023; Accepted October 17, 2023.

This paper was recommended for publication by Editor Clement Gosselin upon evaluation of the Associate Editor and Reviewers' comments.

The authors are with the Department of Engineering Sciences and Methods (DISMI), University of Modena and Reggio Emilia, Italy {federico.benzi,cristian.secchi}@unimore.it

Digital Object Identifier (DOI): see top of this page.

IEEE Robotics and Automation Letters (RA-L) paper, presented at ICRA 2024, Yokohama, Japan. Cite as RA-L paper.

IEEE Robotics and Automation Letters (RA-L) paper, presented at ICRA 2024, Yokohama, Japan. Cite as RA-L paper.

namics accounts for the saturation due to the power valves, thus avoiding an excessive stiffening of the desired behavior and resulting in a compliant interaction with the human. The robust stability of the implemented behavior is guaranteed at all times, owing to an energy tank-based passivity layer.

A similar iterative learning approach has been employed in [21] in a force/impedance controller, but the goal was precise force regulation with unknown environments and there was no adaptation law for the impedance dynamics. In this letter, we address a different control problem (trajectory tracking), as well as investigate and regulate the interplay between variable interactive dynamics, performance and safety in HRC.

Conversely, [19] employs an adaptive control algorithm for varying online the impedance terms in order to track a reference trajectory. While this closely resembles the hereby proposed approach, the structure of the interactive controller and the resulting energy tank interconnection is different, and the values used for the power saturation are fixed *a priori*. Finally, the proposed saturation-aware variation of the admittance dynamics overcomes a dangerous flaw of [19], refining the adaptive algorithm for a safe exploitation in a physical human-robot interaction (pHRI) context.

In summary, the contributions of this paper are:

- an algorithm for passively adapting online the admittance dynamics of a manipulator for improving trajectory tracking performance during an interactive task, while accounting for maximum power saturations;
- an online adaptation law for the injectable power bound, aimed at estimating the minimum power requirement for the task, achieving both safety and efficiency;
- validation of the framework, via both simulations and real experiments with a collaborative manipulator.

The paper is organized as follows: in Sec. II the control task is defined and the problem is formulated. In Sec. III the adaptive admittance controller is presented. Sec. IV outlines the energy tank interconnection. After introducing the power-based safety layer, Sec. V presents the novel online adaptation law of the power bounds and the saturation-aware variation of the admittance dynamics. Simulations and experiments are shown in Sec. VI. Finally, conclusions are drawn in Sec. VII.

II. Problem Formulation

Consider a fully actuated, velocity controlled n-DOFs manipulator modelled via the following kinematic relation:

$$\dot{\boldsymbol{x}} = \boldsymbol{J}(\boldsymbol{q})\dot{\boldsymbol{q}} = \boldsymbol{J}(\boldsymbol{q})\boldsymbol{u}, \tag{1}$$

in which $\dot{\boldsymbol{x}} \in \mathbb{R}^m$, $\boldsymbol{J} \in \mathbb{R}^{m\times n}$, $\boldsymbol{q}$, $\dot{\boldsymbol{q}}$, and $\boldsymbol{u} \in \mathbb{R}^n$ are respectively the operational velocities, the geometric Jacobian, the joint positions and velocities and the control input.

The robot is tasked with physically interacting with unmodelled dynamic objects in the environment via the control wrench $\boldsymbol{w}_c \in \mathbb{R}^m$, moving them around the scene while tracking a reference pose trajectory $\boldsymbol{x}_d \in \mathbb{R}^m$. The interaction is regulated via the following admittance dynamics:

$$\boldsymbol{M}\ddot{\boldsymbol{x}}_{adm} = \boldsymbol{w}_c + \boldsymbol{w}_{ext}, \tag{2}$$

where $\boldsymbol{M} \in \mathbb{R}^{m\times m}$, $\boldsymbol{M} \geq 0$ is the inertia matrix, $\boldsymbol{w}_{ext} \in \mathbb{R}^m$ is the external wrench and $\ddot{\boldsymbol{x}}_{adm}$ is the acceleration of the admittance. By time integration of this last term, the velocity $\dot{\boldsymbol{x}}_{adm}$ of the admittance is synthesized, which is then transformed into a joint velocity set-point $\dot{\boldsymbol{q}}_{adm}$ for the low-level controller of the robot via inverse kinematics. Owing to the highly performing actuation, we can thus assume that the robot reproduces the admittance dynamics, i.e., $\dot{\boldsymbol{x}} \approx \dot{\boldsymbol{x}}_{adm}$.

In order to track the (constant-velocity) reference $\boldsymbol{x}_d$, the control wrench is chosen as the spring-damper dynamics

$$\boldsymbol{w}_c = \boldsymbol{K}_p\tilde{\boldsymbol{x}} + \boldsymbol{K}_d\dot{\tilde{\boldsymbol{x}}}, \tag{3}$$

in which

$$\tilde{\boldsymbol{x}} = \boldsymbol{x}_d - \boldsymbol{x} \tag{4}$$

is the pose error, $\dot{\tilde{\boldsymbol{x}}}$ the velocity error, and $\boldsymbol{K}_p, \boldsymbol{K}_d \in \mathbb{R}^{m\times m}$ are the positive-semidefinite stiffness and damping matrices.

In order to deal with the unmodelled nature of the environment, we modify online the value of the dynamic parameters in (3), such that the resulting command allows to achieve optimal performance, in terms of trajectory tracking error.

Moreover, as the task takes place in a shared workspace, in which physical interaction between the human and the robot can occur, we impose additional safety-related constraints onto the control action, namely:

- ensuring the robust stability of the implemented behavior, both in free motion and in interaction phase;
- limiting the power exertable from the robot to a value which guarantees both safety for the human operator and trajectory tracking performance;
- maintaining the maximum possible degree of compliance, to avoid hazards in case of direct physical interaction with the human operator.

III. Adaptive Admittance Controller

In this Section, we outline the formulation of the variable admittance controller, whose parameter adaptation law stems from the bio-inspired algorithms presented in [22] and [23].

First, we denote as adaptive error the sliding variable [24]

$$\boldsymbol{\varepsilon}(t) = \dot{\tilde{\boldsymbol{x}}}(t) + \delta\tilde{\boldsymbol{x}}(t), \tag{5}$$

with $\delta > 0$. The adaptation law minimizes the tracking error by modifying online the stiffness value in the admittance dynamics, as well as the value of a newly introduced feedforward wrench in the dynamics, aimed at compensating for environmental dynamics, proportionally to $\boldsymbol{\varepsilon}(t)$, as:

$$\dot{\boldsymbol{K}}_p(t) = \boldsymbol{\beta}_p\mathcal{E}(t) - \boldsymbol{\gamma}_p, \tag{6a}$$

$$\dot{\boldsymbol{w}}_{ff}(t) = \boldsymbol{\beta}_f\boldsymbol{\varepsilon}(t) - \boldsymbol{\gamma}_f\boldsymbol{w}_{ff}(t), \tag{6b}$$

in which $\mathcal{E}(t) = diag(|\boldsymbol{\varepsilon}(t)|)$, $\boldsymbol{w}_{ff} \in \mathbb{R}^m$ is the feedforward wrench term [1], while $\boldsymbol{\beta}_p$, $\boldsymbol{\beta}_f \in \mathbb{R}^{m\times m}_{>0}$ are constant diagonal matrices defining the adaptation gain for the stiffness and feedforward term respectively, while $\boldsymbol{\gamma}_p$ and $\boldsymbol{\gamma}_f \in \mathbb{R}^{m\times m}_{>0}$ are corresponding forgetting terms, used to reduced the interactive

[1] Even if the term $\boldsymbol{w}_{ff}$ is computed using the feedback from the error $\boldsymbol{\varepsilon}$, it iteratively learns reproducible forces in the task dynamics, thus acting as a pre-emptive compensation term. Hence, we label it as ”feedforward”.

IEEE Robotics and Automation Letters (RA-L) paper, presented at ICRA 2024, Yokohama, Japan. Cite as RA-L paper.

IEEE Robotics and Automation Letters (RA-L) paper, presented at ICRA 2024, Yokohama, Japan. Cite as RA-L paper.

effort whenever the error gets sufficiently low. These last terms serve to avoid an unnecessary stiffening of the behavior when the task is being correctly implemented.

The value of the damping term is then modified after (6) according to critical damping [25], namely

$$\boldsymbol{K}_d(t) = 2\sqrt{\boldsymbol{K}_p(t)}. \tag{7}$$

The resulting control wrench is thus:

$$\boldsymbol{w}_c(t) = \boldsymbol{K}_p(t)\tilde{\boldsymbol{x}} + \boldsymbol{K}_d(t)\dot{\tilde{\boldsymbol{x}}} + \boldsymbol{w}_{ff}(t). \tag{8}$$

This online adaptation law makes the controller robust to parametric uncertainties, allowing to perform the interaction task even when dealing with unmodelled environments.

IV. Energy Tank Interconnection

A very well known drawback of variable admittance control is the potential loss of passivity [12] and, consequently, of the robust stability of the controller (see [5] for a detailed proof). In this Section, we show how these properties can be recovered via a proper interconnection with the energy tank.

A. Passivity Analysis

Let us start by studying the passivity of the closed-loop system with respect to the power port $(\boldsymbol{w}_{ext}, \dot{\boldsymbol{x}})$, employing as storage function the closed-loop energy function $\mathcal{H}_{cl}$. The energetic contributions in the controller are due to the kinetic energy $\mathcal{H}_{kin}$ and to the elastic term $\mathcal{H}_{spr}$ in (8). However, we do not include the latter in the energy balance, for reasons which we clarify in Remark 1. The energy function is thus:

$$\mathcal{H}_{cl}(t) = \underbrace{\frac{1}{2}\dot{\boldsymbol{x}}^T(t)\boldsymbol{M}\dot{\boldsymbol{x}}(t)}_{\mathcal{H}_{kin}(t)}, \tag{9}$$

The passivity condition imposes that the system does not produce internal energy, i.e., that the following holds:

$$\dot{\mathcal{H}}_{cl} \leq \boldsymbol{w}_{ext}^T\dot{\boldsymbol{x}}. \tag{10}$$

Computing the time derivative of $\mathcal{H}_{cl}$, assuming to keep constant the value of the mass term in (2), we obtain:

$$\dot{\mathcal{H}}_{cl} = \dot{\boldsymbol{x}}^T\boldsymbol{M}\ddot{\boldsymbol{x}}. \tag{11}$$

Leveraging (2) and (8), we can then write:

$$\boldsymbol{M}\ddot{\boldsymbol{x}} = \boldsymbol{K}_p\tilde{\boldsymbol{x}} + \boldsymbol{K}_d\dot{\tilde{\boldsymbol{x}}} + \boldsymbol{w}_{ff} + \boldsymbol{w}_{ext}. \tag{12}$$

Substituting the terms of (12) in (11), we finally get:

$$\begin{aligned}\dot{\mathcal{H}}_{cl} &= \dot{\boldsymbol{x}}^T\boldsymbol{w}_{ext} - \dot{\boldsymbol{x}}^T\boldsymbol{K}_d\dot{\boldsymbol{x}} + \\ &+ \dot{\boldsymbol{x}}^T(\underbrace{\boldsymbol{K}_p\tilde{\boldsymbol{x}} + \boldsymbol{K}_d\dot{\boldsymbol{x}}_d + \boldsymbol{w}_{ff}}_{\bar{\boldsymbol{w}}_c}).\end{aligned} \tag{13}$$

From this balance, we group all the possibly active terms in $p = \dot{\boldsymbol{x}}^T\bar{\boldsymbol{w}}_c$ and isolate the dissipative term $d = \dot{\boldsymbol{x}}^T\boldsymbol{K}_d\dot{\boldsymbol{x}}$.

B. Energy Tank Interconnection

In order to preserve passivity at all times, we interconnect the controller to a virtual energy tank, augmenting the closed loop dynamics. Energy tanks store the energy of the system via a properly designed interconnection, serving as energy reservoirs. Their general representation is as follows:

$$\begin{cases}\dot{x}_t(t) = u_t(t) \\ y_t(t) = \frac{\partial T}{\partial x_t} = x_t(t),\end{cases} \tag{14}$$

in which $x_t(t) \in \mathbb{R}$ is the state of the tank, $(u_t(t), y_t(t)) \in \mathbb{R} \times \mathbb{R}$ is the input-output power port, while

$$T(x_t(t)) = \frac{1}{2}x_t(t)^2 \tag{15}$$

is the energy stored in the tank. This energy reservoir can then be re-utilized for passively implementing any control action, by designing the tank input such that the active terms are compensated and the dissipated power is stored, namely:

$$u_t(t) = \varphi\left(\frac{\eta}{x_t}\dot{\boldsymbol{x}}^T\boldsymbol{K}_d\dot{\boldsymbol{x}} - \frac{\dot{\boldsymbol{x}}^T\bar{\boldsymbol{w}}_c}{x_t}\right), \tag{16}$$

where $\varphi \in [0, 1]$ enables/disables the energy storing process (see, e.g., [26]), while the gain $\eta \in [0, 1]$ allows to control how much of the dissipated power is stored into the tank. By (16) and (14), the tank power flow $\dot{T}$ can be computed as:

$$\dot{T} = x_t\dot{x}_t = x_t u_t = \varphi\eta\dot{\boldsymbol{x}}^T\boldsymbol{K}_d\dot{\boldsymbol{x}} - \dot{\boldsymbol{x}}^T\bar{\boldsymbol{w}}_c = \varphi\eta d - p. \tag{17}$$

Proposition 1. *If* $T(t) > 0\,\forall t \geq 0$*, then the system* (2) *interconnected with the energy tank* (14) *via* (16) *is passive.*

Proof. Since $T(t) > 0$, then $x_t \neq 0$, meaning (16) is always well defined. Consider the total energy of the closed-loop system augmented with the energy tank $\bar{\mathcal{H}}_{cl} = \mathcal{H}_{cl} + T$. Making use of (17) we have that:

$$\begin{aligned}\dot{\bar{\mathcal{H}}}_{cl} &= \dot{\mathcal{H}}_{cl} + \dot{T} = -d + \dot{\boldsymbol{x}}^\top\boldsymbol{w}_{ext} + p + \dot{T} \\ &= -(1 - \eta\varphi)d + \dot{\boldsymbol{x}}^\top\boldsymbol{w}_{ext} \leq \dot{\boldsymbol{x}}^\top\boldsymbol{w}_{ext}.\end{aligned} \tag{18}$$

where the inequality comes from the fact that $\varphi, \eta \leq 1$. □

From the passivity of the controller, we can thus infer the robust stability of the overall system while interacting with any external environment (see, e.g., [5], [10]).

In order to avoid the implementation of practically unstable actions [27], the amount of energy to be allocated for task execution has to be finite. Thus, an upper and lower bound for the energy in the tank, respectively T^+ and T^-, must be enforced. To this end, we set $0 < T^- < T^+$ and halt the energy injection as $T(t) = T^+$ by setting $\varphi = 0$.

V. Unified Power & Admittance Adaptation

Since bounding the amount of energy allocated for task execution is not sufficient for ensuring safety in HRC, in this Section we exploit the concepts of *power valves* [17] for limiting the rate of energy extraction from the tank.

IEEE Robotics and Automation Letters (RA-L) paper, presented at ICRA 2024, Yokohama, Japan. Cite as RA-L paper.

IEEE Robotics and Automation Letters (RA-L) paper, presented at ICRA 2024, Yokohama, Japan. Cite as RA-L paper.

A. Power Valves

Consider the non-passive control action $\bar{\boldsymbol{w}}_c$ in (13). We can modulate its associated power flow p by applying a scaling factor $\boldsymbol{\Gamma} = diag(\gamma_1, \dots, \gamma_m)$, i.e.,

$$\gamma_i = \begin{cases} \frac{p_i^+}{p_i} & \text{if } p_i > p_i^+, \\ 1 & \text{otherwise,} \end{cases} \tag{19}$$

in which $p_i = \dot{x}_i w_{c,i}$, $p_i \in \mathbb{R}$, is the power injected along the $i-$th direction and $\boldsymbol{p}^+ \in \mathbb{R}^m$ contains the maximum power value for each operational direction. The scaling factor is then applied directly in the tank input (16):

$$u_t^*(t) = \varphi \left(\frac{\eta}{x_t} \dot{\boldsymbol{x}}^T \boldsymbol{K}_d \dot{\boldsymbol{x}} - \frac{\dot{\boldsymbol{x}}^T \boldsymbol{\Gamma} \bar{\boldsymbol{w}}_c}{x_t} \right), \tag{20}$$

The power flow scaling process results in the saturation of $\bar{\boldsymbol{w}}_c$, allowing us to rewrite the control wrench in (8) as:

$$\boldsymbol{w}_c^* = \boldsymbol{\Gamma} \bar{\boldsymbol{w}}_c - \boldsymbol{K}_d \dot{\boldsymbol{x}}. \tag{21}$$

Remark 1. *While the previous choices for the energy function* (9) *and power port in Sec. IV-A might appear conservative (only the time-varying spring energy in $\mathcal{H}_{spr}$ needs to be compensated for preserving passivity [20]), they allow us to encompass all the terms which can undermine human safety (i.e., $\bar{\boldsymbol{w}}_c$) inside the tank input* (16). *In this way, by simply acting upon the energy flows at the port of the tank, we can superintend the entire interactive behavior of the controlled system, enforcing safety as we deem necessary.*

Finally, the valve gain is multiplied by a factor $\alpha \in [0, 1]$[2] such that $\boldsymbol{\Gamma}^* = \alpha \cdot \boldsymbol{\Gamma}$, which halts the power harvesting from the tank whenever $T = T^-$, avoiding singularities in (16).

B. Power Bound Adaptation Law

Opportunely setting the maximum power bounds $\boldsymbol{p}^+$ is pivotal in achieving both safety and effectiveness during task execution. Since a proper *a priori* choice for these values cannot be found, due to the unmodelled nature of the environment, we propose an adaptation algorithm aimed at estimating online the necessary power bound for effective task execution. As our control goal is trajectory tracking, we modify the previously presented algorithm in [21], tailoring it to our needs. The newly proposed adaptation law is:

$$\dot{\boldsymbol{p}}^+(t) = (\boldsymbol{I}_m - \boldsymbol{\Gamma}) \boldsymbol{\beta}_c |\boldsymbol{\varepsilon}(t)| - \boldsymbol{\gamma}_c \boldsymbol{1}_m, \tag{22}$$

in which, resembling the terms in (6), $\boldsymbol{\beta}_c, \boldsymbol{\gamma}_c \in \mathbb{R}^{m \times m}_{>0}$ serve as adaptation and forgetting factors respectively. This novel formulation allows to modify online each power bound according to the value of the adaptive error along that direction, as well as the current degree of valve saturation. In this way, if the initially set bound does not allow to achieve optimal tracking performance, the algorithm will increases the maximum exertable power. The forgetting factor $\boldsymbol{\gamma}_c$ allows then to reduce this value whenever a sufficiently small $\boldsymbol{\varepsilon}(t)$ is achieved. The value of $\boldsymbol{p}^+$ then settles to the minimal one

[2] Both α and φ are varied smoothly using a shaping function when approaching T^- and T^+, similarly to [14], [18], thus avoiding discontinuities.

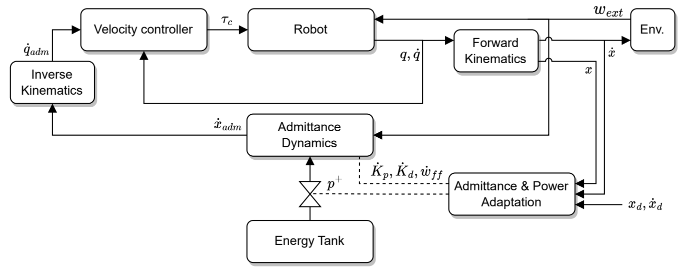

Fig. 2: The overall architecture. We assume that the actuation of the robot is performing enough that the torques applied by the low-level controller $\boldsymbol{\tau}_c$ allow to reproduce the set-point, i.e., $\dot{\boldsymbol{q}} = \dot{\boldsymbol{q}}_{adm}$.

necessary for achieving optimal trajectory tracking, avoiding excessive power flows in the system.

Furthermore, if any application-dependent limits onto the exertable power $\boldsymbol{p}_{max}$ are known, e.g., from technical specifications or from risks assessment procedures (see, e.g., [28]), these can be embedded directly into the adaptation law (22), ensuring via additional parameters that $\boldsymbol{p}^+ \leq \boldsymbol{p}_{max}$.

C. Saturation-Aware Admittance Adaptation

As in [19], the stiffness and force terms in (6) are varied independently of the power scaling factor. In case of sub-optimal tracking performance due to power-related wrench saturation, the algorithm leads to an excessive build-up of stiffness and reference force terms in the controller, as the error variable would not converge to zero. This results in unwanted aggressive behaviors whenever the power-based wrench saturation is not active, namely when the robot is stopped or slowed down due to, e.g, an interaction with the human or the environment. In order to overcome this issue, we propose to embed the power-based saturation directly into the dynamics adaptation law. This allows to simultaneously:

- avoid unnecessary build-up of force and stiffness in the admittance, which could lead to unsafe and oscillatory behaviors whenever the valve saturation is not active;
- reduce the parameter dependency of the controller, as the effect of the learning hyper-parameters in (6) is modulated by the power-based safety layer.

To this end, we propose to further modify the dynamic parameters according to the degree of valve saturation. This allows us to couple the power-based safety layer and the admittance adaptation law, making the latter aware of the saturation process. Thus, the novel saturation-aware adaptive laws for the admittance dynamics are formulated as follows:

$$\dot{\boldsymbol{K}}_p^*(t) = \boldsymbol{\Gamma} \boldsymbol{\beta}_p \mathcal{E} - \boldsymbol{\gamma}_p, \tag{23a}$$

$$\dot{\boldsymbol{w}}_{ff}^*(t) = \boldsymbol{\Gamma} \boldsymbol{\beta}_f \boldsymbol{\varepsilon}(t) - \boldsymbol{\gamma}_f \boldsymbol{w}_{ff}. \tag{23b}$$

The adaptation laws in (23) simultaneously achieve performance, compliance and safety, reflecting the requirements of the novel context (pHRI) in which the control architecture is deployed. The final overall architecture is portrayed in Fig. 2.

VI. Simulations and Experiments

The presented architecture has been extensively validated both via simulations and experimentally onto a collaborative

IEEE Robotics and Automation Letters (RA-L) paper, presented at ICRA 2024, Yokohama, Japan. Cite as RA-L paper.

Parameter	Value
$\boldsymbol{M}$	$[7 \quad 7 \quad 7 \quad 0.5 \quad 0.5 \quad 0.5] kg$
$\boldsymbol{K}_{p,0}$	$[20 \quad 20 \quad 20 \quad 1 \quad 1 \quad 1] \frac{N}{m}$
$\boldsymbol{K}_d$	Critical damping [25]
δ	5
$\boldsymbol{\beta}_p$	$[0 \quad 80 \quad 0 \quad 0 \quad 0 \quad 0]$
$\boldsymbol{\gamma}_p$	$[0 \quad 8 \quad 0 \quad 0 \quad 0 \quad 0]$
$\boldsymbol{\beta}_f$	$[0 \quad 200 \quad 0 \quad 0 \quad 0 \quad 0]$
$\boldsymbol{\gamma}_f$	$[0 \quad 10 \quad 0 \quad 0 \quad 0 \quad 0]$
η	0
$\boldsymbol{\beta}_c$	$[0 \quad 0.4 \quad 0 \quad 0 \quad 0 \quad 0]$
$\boldsymbol{\gamma}_c$	$[0 \quad 0.33 \quad 0 \quad 0 \quad 0 \quad 0]$

TABLE I: Control and Learning Parameters used in the Validation. For diagonal matrices, only the entries on the diagonal are reported.

manipulator. The employed robot is a 6DOF Universal Robot 10e controlled at a rate of $500Hz$ and endowed with a F/T sensor at the end effector, running at the same frequency. The chosen interaction task consists in pushing an unmodelled object, tracking a desired trajectory $\boldsymbol{x}_d$. As in related works on the topic (see, e.g., [17]–[20]), we consider only translational motions for the validation process, since these are most likely to threaten the safety of the application. Nevertheless, the proven results still hold for more complex interactive tasks, due to the generality of the framework.

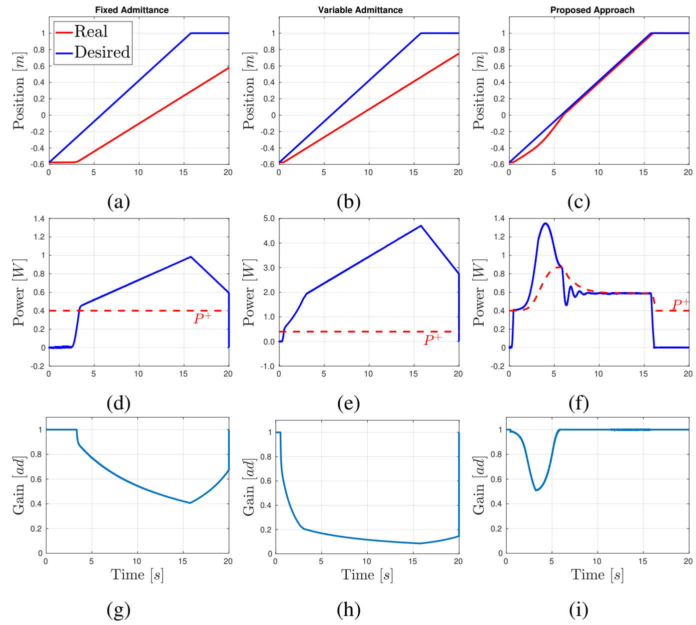

Fig. 3: Simulation results comparing the proposed approach with the adaptive controller in [19] and the standard admittance controller.

A. Simulations with UR10e

In the set of simulations, conducted in CoppeliaSim environment, the collaborative manipulator is tasked with pushing a box of unknown mass and friction (real values $m_{obj} = 2kg$ and $\mu_{obj} = 0.3$ [3]) for a distance of $1.57m$ along its Y-axis, moving at a constant speed of $\dot{x}_{d,2} = 0.1\frac{m}{s}$.

The task is first performed using the standard admittance controller (3), then using the variable admittance algorithm (8) proposed in [19], and finally with the adaptive architecture presented in this letter. In the first two cases, a fixed power limit $p_2^+ = 0.4W$ is set, according to the partial knowledge of the task and an initial estimate of the environmental model. For the last simulation, this initial bound is modified online according to (22). Additional parameters are listed in Table I.

The results of this comparative study are presented in Fig. 3, which portrays the desired and actual pose of the robot, the power p_2 requested from the controller and the maximum bound p_2^+, and the valve gain γ_2 for each employed controller.

Due to the unmodelled nature of the environment, resulting in a poor initialization of the fixed stiffness value $\boldsymbol{K}_{p,0}$, the standard admittance controller initially fails to push the obstacle along the trajectory. Even once the commanded force grows large enough to overcome the friction effect and the system starts moving, the performance are still sub-optimal, as the saturation induced by the valve limits the maximum applicable power. Notice how even the standard controller can lead to unsafe behaviors (i.e., high power requests), supporting our choices in Sec. IV-A (see Rmk. 1).

The simulations with the second architecture showcase that, while varying the admittance dynamics ensures an initially prompt reaction, a poor choice for the fixed power bound can severely affect task performance, as it forbids the system from properly tracking the desired reference. Additionally, the continuous increase of the adaptive error $\boldsymbol{\varepsilon}(t)$ leads to an excessive buildup of stiffness and force in the controller over time. This is reflected in Fig. 3e, in which the requested power reaches dangerous values ($\sim 5W$), resulting in the aggressive valve saturation shown in Fig. 3h. These results prove how strong of an effect the power saturation has onto task execution, how hard it is to find a suitable power bound, and how unfit [19] is for a collaborative application.

By varying online the power bound via (22), the newly proposed approach manages to significantly improve the tracking performance. After an initial overshoot, necessary to compensate the momentary deviation from the set-point, the value of the power bound converges precisely to the nominal one required for optimal task execution (see Fig. 3f). Consequently, the valve gain in Fig. 3i settles to a unitary value. Thus, the novel control architecture manages to estimate online and allocate to the system precisely the necessary power budget, achieving both safety and efficiency.

Furthermore, the addition of the saturation terms in (23), together with the fact that the reference trajectory is better tracked, allows to strongly reduce the force resulting from the admittance dynamics. The value of the desired and saturated admittance parameters, together with the resulting interaction force, is portrayed in Fig. 4 (second and third simulations only). As will be shown in the following experiments, this saturation-aware adaptation of the interactive parameters is pivotal in maximizing compliance in HRC scenarios.

Finally, the boxplots in Fig. 5 report the distribution of the adaptive error during the simulations for each approach. While modifying online the admittance dynamics alone leads to a noticeable performance improvement, the fixed bound onto the extractable power from the tank still severely limits the capabilities of the controller. The novel architecture hereby presented allows to overcome this issue, thus significantly outperforming both the previous controllers.

[3] We hereby assume the friction to be purely Coulombian and dynamic.

IEEE Robotics and Automation Letters (RA-L) paper, presented at ICRA 2024, Yokohama, Japan. Cite as RA-L paper.

IEEE Robotics and Automation Letters (RA-L) paper, presented at ICRA 2024, Yokohama, Japan. Cite as RA-L paper.

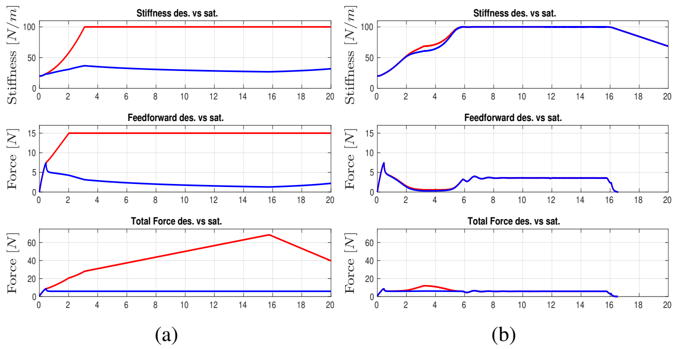

Fig. 4: Simulation results showcasing the effect of the saturation-aware variation of the admittance terms. In *red* the pre-saturated values of stiffness, feedforward force and total interaction force. In *blue* the post-saturation, i.e., the implemented ones.

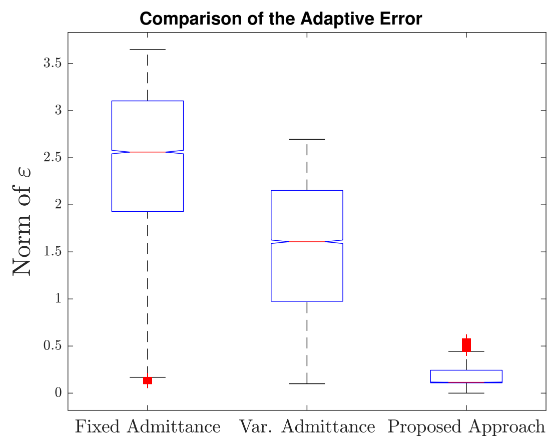

Fig. 5: Boxplots showcasing the distribution of the adaptive error using the different approaches for the simulated robot.

B. Experiments with UR10e

The experimental validation of the novel control architecture consists in the aforementioned pushing task, implemented with the three different approaches, alongside an evaluation of the degree of compliance and safety guaranteed by the controller in a HRC scenario. The experimental setup is showcased in Fig. 1, alongside the reference frame used.

Fig. 6 showcases the outcome of the comparative study, while Fig. 7 presents the distribution of the adaptive error for each controller. The experimental results mirror those previously reported for the simulated robot, thus validating the capabilities of our novel architecture also in realistic scenarios, characterized by more complex interactive behaviors (due, e.g., to non-purely Coulombian friction forces).

As a final step of the validation process, we evaluate the behavior of the robot when physically interacting with the human, comparing the previous adaptive controller [19] with the one proposed in this letter. During the execution of the pushing task, the operator interferes by applying a force $\boldsymbol{w}_{ext}$ to the transported object, with the intention of reversing its motion. As the velocity of the robot gradually decreases, the saturation due to the power valve halts, allowing the direct implementation of the active wrench $\bar{\boldsymbol{w}}_c$. Using the previous adaptive controller, this results in a severely stiff interactive behavior, caused by the aforementioned progressive buildup of the dynamic parameters. This results in the impossibility for the operator to reverse the motion of the robot, even when applying a noticeable force to the system.

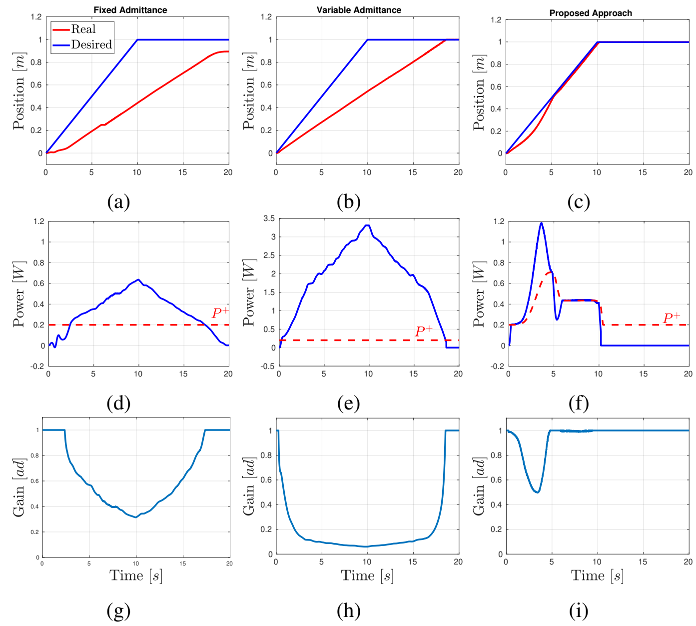

Fig. 6: Experimental results from the comparative study conducted with the real robot.

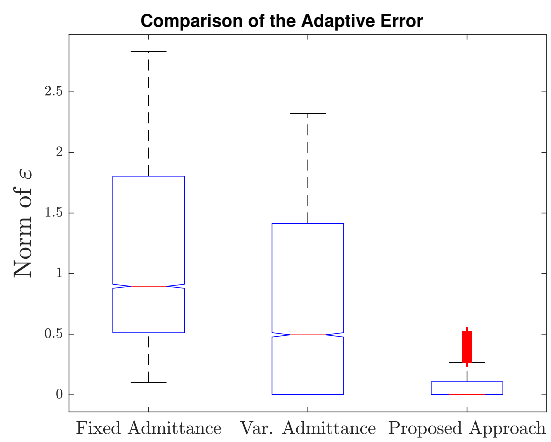

Fig. 7: Boxplots showcasing the distribution of the adaptive error using different approaches in the experiments with the real robot.

Conversely, the novel saturation-aware adaptive law (23) allows to maintain significantly lower values for both stiffness and feedforward force during the motion. This translates into a more compliant interactive behavior and allows the human operator to reverse the motion of the robot, as well as reducing the necessary effort. During these transients of opposite motion, the adaptive error $\boldsymbol{\varepsilon}(t)$ grows noticeably, thus resulting in a quick stiffening of the behavior. Nevertheless, during each interaction phase, the control force remains significantly lower than the one induced with the previous controller, meaning that the operator is always able to push the robot away.

The results of this final HRC experiment are presented in Fig. 8. Additional informative plots regarding the experimental validation can be found in the accompanying video.

IEEE Robotics and Automation Letters (RA-L) paper, presented at ICRA 2024, Yokohama, Japan. Cite as RA-L paper.

IEEE Robotics and Automation Letters (RA-L) paper, presented at ICRA 2024, Yokohama, Japan. Cite as RA-L paper.

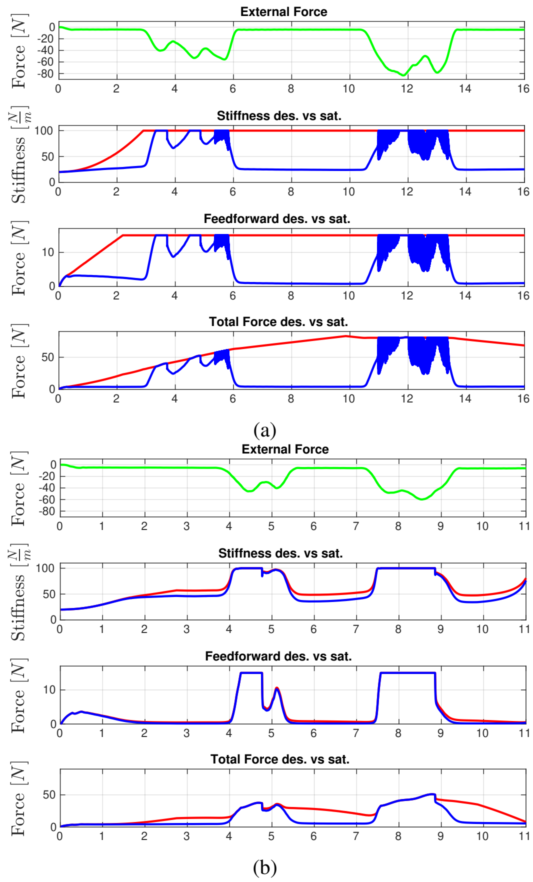

Fig. 8: Results from the collaborative experiment. The buildup of stiffness and force using [19] reduces compliance and might lead to hazardous scenarios for the human operator during the interaction.

VII. Conclusions and Future Works

In this paper, we introduced an adaptive framework for passively accomplishing a desired interaction task, focusing on estimating online the correct power bound for achieving simultaneously high-level safety in HRC scenarios and trajectory tracking performance. The proposed architecture outperformed the previous controllers under both aspects. Future works aim at combining both energy and power adaptation laws for providing a unified safety framework for collaborative tasks.

References

[1] X. Liu, S. S. Ge, F. Zhao, and X. Mei, "Optimized impedance adaptation of robot manipulator interacting with unknown environment," *IEEE Transactions on Control Systems Technology*, vol. 29, no. 1, pp. 411–419, 2020.

[2] S. Hwang, S. H. Park, M. Jin, and S. H. Kang, "A robust control of robot manipulators for physical interaction: stability analysis for the interaction with unknown environments," *Intelligent Service Robotics*, vol. 14, no. 3, pp. 471–484, 2021.

[3] A. Meguenani, V. Padois, J. Da Silva, A. Hoarau, and P. Bidaud, "Energy based control for safe human-robot physical interaction," in *2016 International Symposium on Experimental Robotics*. Springer, 2017, pp. 809–818.

[4] E. Franco, T. Ayatullah, A. Sugiharto, A. Garriga-Casanovas, and V. Virdyawan, "Nonlinear energy-based control of soft continuum pneumatic manipulators," *Nonlinear Dynamics*, vol. 106, pp. 229–253, 2021.

[5] S. Stramigioli, "Energy-aware robotics," in *Mathematical Control Theory I*. Springer, 2015, pp. 37–50.

[6] C. Secchi, S. Stramigioli, and C. Fantuzzi, *Control of interactive robotic interfaces: A port-Hamiltonian approach*. Springer Science & Business Media, 2007, vol. 29.

[7] A. Van der Schaft, *L2-gain and passivity techniques in nonlinear control*. Springer, 2000.

[8] A. Franchi, C. Secchi, H. I. Son, H. H. Bulthoff, and P. R. Giordano, "Bilateral teleoperation of groups of mobile robots with time-varying topology," *IEEE Transactions on Robotics*, vol. 28, no. 5, pp. 1019–1033, 2012.

[9] L. Sabattini, C. Secchi, B. Capelli, and C. Fantuzzi, "Passivity preserving force scaling for enhanced teleoperation of multirobot systems," *IEEE Robotics and Automation Letters*, vol. 3, no. 3, pp. 1925–1932, 2018.

[10] F. Benzi, F. Ferraguti, G. Riggio, and C. Secchi, "An energy-based control architecture for shared autonomy," *IEEE Transactions on Robotics*, vol. 38, no. 6, pp. 3917–3935, 2022.

[11] F. Ficuciello, L. Villani, and B. Siciliano, "Variable impedance control of redundant manipulators for intuitive human–robot physical interaction," *IEEE Transactions on Robotics*, vol. 31, no. 4, pp. 850–863, 2015.

[12] F. Benzi and C. Secchi, "An optimization approach for a robust and flexible control in collaborative applications," in *2021 IEEE International Conference on Robotics and Automation (ICRA)*. IEEE, 2021, pp. 3575–3581.

[13] F. Califano, R. Rashad, C. Secchi, and S. Stramigioli, "On the use of energy tanks for robotic systems," in *Human-Friendly Robotics 2022: HFR: 15th International Workshop on Human-Friendly Robotics*. Springer, 2023, pp. 174–188.

[14] C. Schindlbeck and S. Haddadin, "Unified passivity-based cartesian force/impedance control for rigid and flexible joint robots via task-energy tanks," in *2015 IEEE international conference on robotics and automation (ICRA)*. IEEE, 2015, pp. 440–447.

[15] R. Rashad, D. Bicego, J. Zult, S. Sanchez-Escalonilla, R. Jiao, A. Franchi, and S. Stramigioli, "Energy aware impedance control of a flying end-effector in the port-hamiltonian framework," *IEEE transactions on robotics*, vol. 38, no. 6, pp. 3936–3955, 2022.

[16] M. Risiglione, J.-P. Sleiman, M. V. Minniti, B. Cizmeci, D. Dresscher, and M. Hutter, "Passivity-based control for haptic teleoperation of a legged manipulator in presence of time-delays," in *2021 IEEE/RSJ International Conference on Intelligent Robots and Systems (IROS)*. IEEE, 2021, pp. 5276–5281.

[17] E. Shahriari, L. Johannsmeier, and S. Haddadin, "Valve-based virtual energy tanks: A framework to simultaneously passify controls and embed control objectives," in *2018 Annual American Control Conference (ACC)*. IEEE, 2018, pp. 3634–3641.

[18] M. Brunner, L. Giacomini, R. Siegwart, and M. Tognon, "Energy tank-based policies for robust aerial physical interaction with moving objects," *arXiv preprint arXiv:2202.06755*, 2022.

[19] F. Benzi, M. Brunner, M. Tognon, C. Secchi, and R. Siegwart, "Adaptive tank-based control for aerial physical interaction with uncertain dynamic environments using energy-task estimation," *IEEE Robotics and Automation Letters*, vol. 7, no. 4, pp. 9129–9136, 2022.

[20] Y. Michel, C. Ott, and D. Lee, "Safety-aware hierarchical passivity-based variable compliance control for redundant manipulators," *IEEE Transactions on Robotics*, vol. 38, no. 6, pp. 3899–3916, 2022.

[21] E. Shahriari, L. Johannsmeier, E. Jensen, and S. Haddadin, "Power flow regulation, adaptation, and learning for intrinsically robust virtual energy tanks," *IEEE Robotics and Automation Letters*, vol. 5, no. 1, pp. 211–218, 2020.

[22] Y. Li, G. Ganesh, N. Jarrassé, S. Haddadin, A. Albu-Schaeffer, and E. Burdet, "Force, impedance, and trajectory learning for contact tooling and haptic identification," *IEEE Transactions on Robotics*, vol. 34, no. 5, pp. 1170–1182, 2018.

[23] G. Ganesh, A. Albu-Schäffer, M. Haruno, M. Kawato, and E. Burdet, "Biomimetic motor behavior for simultaneous adaptation of force, impedance and trajectory in interaction tasks," in *2010 IEEE International Conference on Robotics and Automation*. IEEE, 2010, pp. 2705–2711.

[24] J.-J. E. Slotine, "Sliding controller design for non-linear systems," *International Journal of control*, vol. 40, no. 2, pp. 421–434, 1984.

[25] C. Ott, *Cartesian impedance control of redundant and flexible-joint robots*. Springer, 2008.

[26] M. Minelli, N. Piccinelli, F. Falezza, F. Ferraguti, R. Muradore, and C. Secchi, "Two-layer-based multiarms bilateral teleoperation architecture," *IEEE Transactions on Control Systems Technology*, 2022.

[27] D. Lee and K. Huang, "Passive-set-position-modulation framework for interactive robotic systems," *IEEE Transactions on Robotics*, vol. 26, no. 2, pp. 354–369, 2010.

[28] C. Harper and G. Virk, "Towards the development of international safety standards for human robot interaction," *International Journal of Social Robotics*, vol. 2, no. 3, pp. 229–234, 2010.

IEEE Robotics and Automation Letters (RA-L) paper, presented at ICRA 2024, Yokohama, Japan. Cite as RA-L paper.